?5-20

393888

358110

1997

NASA/ASEE SUMMER FACULTY FELLOWSHIP PROGRAM

MARSHALL SPACE FLIGHT CENTER
THE UNIVERSITY OF ALABAMA IN HUNTSVILLE

1-D NUMERICAL ANALYSIS OF RBCC ENGINE PERFORMANCE

Prepared By:	Samuel S. Han
Academic Rank:	Professor
Institution and Department:	Tennessee Technological University Department of Mechanical Eng.
NASA/MSFC:	
Branch:	Combustion Physics
Division:	Engine Systems
Laboratory:	Propulsion
MSFC Colleague:	S. Don Bai, Ph.D.

Introduction

RBCC engine combines air breathing and rocket engine into a single engine to increase the specific impulse over an entire flight trajectory. Considerable research pertaining to RBCC propulsions was performed during 1960's and these engines were revisited recently as a candidate propulsion system for either a single-stage-to-orbit (SSTO) or two-stage-to-orbit (TSTO) launch vehicle (Foster, et. al., 1988). There are variety of RBCC configurations that had been evaluated and new designs are currently under development. However, the basic configuration of all RBCC systems is built around the ejector scramjet engine originally developed for hypersonic airplane. In this configuration, a rocket engine plays as an ejector in the air-augmented initial acceleration mode, as a fuel injector in scramjet mode and the rocket in all rocket mode for orbital insertion (Escher, 1995).

Computational fluid dynamics (CFD) is a useful tool for the analysis of complex transport processes in various components in RBCC propulsion systems. The objective of the present research was to develop a transient 1-D numerical model that could be used to predict flow behavior throughout a generic RBCC engine following a flight path.

1-D Numerical Model

One dimensional transient compressible flow equations used in the model are mass, linear momentum and energy equations. They are :

$$\frac{\partial \rho A}{\partial t}+\frac{\partial \rho u A}{\partial x}=m_{inj}A$$

$$\frac{\partial \rho u A}{\partial t}+\frac{\partial}{\partial x}\left[A\left\{\rho uu-(2\mu+\lambda)\frac{\partial u}{\partial x}\right\}\right]=-A\frac{\partial p}{\partial x}-\tau_w p_w+m_{inj}Au_{inj}$$

$$\frac{\partial \rho u e}{\partial t}+\frac{\partial}{\partial x}\left[A\left(\rho u e-\kappa\frac{\partial T}{\partial x}\right)\right]=-p\frac{\partial u A}{\partial x}+u\tau_w p_w+m_{inj}h_{inj}A+q_{gen}A+uu_{inj}m_{inj}A-1.5u^2m_{inj}A$$

In these equations, ρ density, u velocity, p pressure, e internal energy, x axial coordinate , t time, and A(x,t) is the cross-sectional area. Ejector mass flow rate, m_{inj}, was the primary rocket mass flow rate, and h_{inj}, was calculated by using primary rocket nozzle exit temperature and Cp of the primary rocket combustion products. Exit velocity of the gas at the primary rocket nozzle, u_{inj}, was calculated via ideal gas equation with known primary rocket exit pressure and exit area. Energy release from hydrogen injection, q_{gen}, was treated as uniform energy input. Stoichiometric reaction of hydrogen and oxygen was assumed.

For the present study, molecular viscosity of the fluid, μ and λ, are negligible and therefore wall friction was neglected. τ_w represents minor losses due to sudden area change modeled after incompressible flow case,

$$\tau_w = c_d \frac{1}{2} \rho u^2$$

where c_d is a form drag coefficient ranging from 0.05 to 0.2 and p_w is the wetted perimeter of the cross section.

Numerical scheme used was a variant of SIMPLE method that incorporates compressibility of the fluid. A staggered grid was used. Time accuracy of the solution was obtained by choosing time steps slightly larger than those dictated by CFL conditions. Mass, momentum and energy addition from primary rocket and hydrogen injectors were uniformly distributed over the chosen control volumes using source term linearization.

Imposition of numerical boundary conditions depend not only on the nature of the problems but also on the numerical methods used and often creates erroneous solutions. In RBCC operation, primary rocket was used to initiate the flow and thus disturbance to the initially static condition in the engine began internally and propagated to the inlet and exit of the engine. At the engine inlet, static pressure was extrapolated by using static pressures next to inlet boundary. The remaining flow properties were then calculated by using free stream conditions assuming that the process from the free stream to the inlet was isentropic. If there was a shock ahead of the inlet, flow properties of the free stream must be readjusted accordingly. This step was not taken in the present calculation. At the end of the exit nozzle, atmospheric pressure was imposed if the flow at the exit was subsonic and extrapolated pressure was used otherwise.

Simulation Results

Table 1 shows bypass ratio of an ideal ejector calculated by the present numerical model in comparison with analytical solution (Heiser and Pratt, 1994). Numerical results agreed well with the analytical solution up to free stream Mach number 1.0. Results deviated rapidly with increasing free stream Mach number beyond 1.0. In the numerical model, primary flow pressure and the induced air flow pressures were not assumed equal at the inlet plane of the mixer while they were assumed equal in analytical method.

Table 1. Ideal Ejector Bypass Ratio

Free stream Mach no	Numerical	Analytical
0.0	1.65	1.68
0.5	1.94	1.92
1.0	2.98	2.93
1.5	4.47	5.66
2.0	6.00	12.10

Another calculations were performed to obtain the bypass ratio and the ejector stagnation pressure ratio for the Pratt-Whitney test rig. Numerical results obtained by the present model for three free stream Mach numbers following a flight trajectory were compared with the results RJPA code of John Hopkins University. A reasonable agreement was obtained. This was expected since both models were based on the same equations except the time dependent terms in the present model.

To validate the accuracy of the numerical model, numerical results were next compared with the test data. Test data of a duel-mode ejector scramjet engine developed by Marquardt (Congelliere, et. al., 1968) was used for that purpose. Fig. 1 shows flow area along the axis of the engine; diverging inlet, combuster and after-burner-exit nozzle and constant area mixer (ejector). Flow areas were changed abruptly at the strut and where pressure probes were located. Free stream Mach numbers were varied from 0 to 6.0. Test results were presented in terms of pressures and induced air flow rate. A bell mouth was placed at the inlet for the static test only.

Fig. 2 shows the static pressure distributions for four cases along the engine at $M_0=0$. Flow speed remained subsonic throughout the engine. Experimental wall pressure distribution (broken line) showed static pressure was increased through the ejector, decreased in the constant area mixer, increased in the combustor and further increased through the after-burner-exit nozzle. Sharp pressure changes due to the presence of pressure probes were apparent. Ideal case (-Δ-) assumed no form drag due to area changes and the mixer area was assumed constant as the actual geometry. Without form drag, pressure at the inlet was much lower than the test data and no pressure bumps were shown at the probe locations. Since the flow was subsonic, pressure in the constant area mixer remained constant and increased smoothly through the diverging part of the remaining engine. Tested pressure in the mixer, however, decreased rapidly along the mixer indicating that the flow accelerated in the mixer. This implies that active cross sectional area of the mixer was progressively reduced. This is similar to accelerating flow through an isolator in a dual-mode scramjet engine. A supersonic flow (Heiser and Pratt, 1994) entering a constant area isolator remains supersonic at the mixer outlet because of reduced flow area. Active flow area decreases because of boundary layer that is generated by series of oblique shocks. Isolator acts as a buffer when the engine switches from a ramjet to a scramjet modes in a dual-mode scramjet engine. In ejector mode, flow in the mixer is subsonic but oblique shocks are created by the high pressure primary flow and the low pressure induced air flow (Daines, 1995). The exit area of the mixer was thus reduced by 20 % in subsequent calculations and the results showed a better agreement with the test data. Overall pressure distribution was higher with a form drag ($c_d=0.05$) than without. Even without a form drag, numerical results were higher than the test data. This might be explained by the fact that measured pressure was wall pressure which was much lower than the pressure at the center of the mixer. Numerical results were obtained at free stream Mach numbers, 0.8, 1.6 and 3.0 without hydrogen injections. Table 2 shows the bypass ratios calculated by ideal ejector analysis and the present model in comparison with the test data.

Fig. 3 shows the effects of hydrogen injections at two locations: "A" at the end of combustor and "B" at the beginning of combustor. Injection of hydrogen was 0.0165 kg/s and a stoichiometric reaction with oxygen in the induced air was assumed.

Table 2. Bypass Ratio for Marquardt Test Engine

M_0	Ideal (H&P)	Numerical (w/o drag)	Numerical (w drag)	Test data
0.0	5.14	3.6	3.6	2.67
0.8	7.81	5.4	4.2	5.01
1.6	21.61	14.43	10.76	12.5

Energy release in the combustion chamber increased the static pressure before the injection points and caused flow acceleration and rapid pressure drop after injection points as expected in a subsonic flow. Pressure distribution however agreed only qualitatively with the test data. Fig. 4 shows pressure and Mach number distributions with "A" injection and without injection at M_0=3.0. Again with injection pressure increased and the flow became subsonic before the injection point and choked in the after-burner followed by supersonic expansion. This is an example of ramjet mode operation. Without hydrogen injection, flow is choked at the end of mixer and the flow become supersonic in the combustor (M=1.5) and remained supersonic.

Conclusions and Recommendations

A transient 1-D numerical model was used to study fundamental mechanisms involved in RBCC propulsion systems. Numerical results obtained by the present model for the ejector mode agreed well with other available analytical data. Comparison with test data showed that inlet interactions, mixing processes in the ejector and energy release in the combustor have dominant effects on the performance of the engine. Additional studies are recommended for the inlet interactions, and the chemical reactions in the combustor before simulating modes transition following a actual flight path and parametric study on various engine configurations.

References

Congelliere, J., Prevatte, N., and Lime, J., Advanced Ramjet Concepts: Volume 2-Ejector Scramjet Technology, AFAPL-TR-67-118, Vol.2, 1968.

Daines, R. L., Computational Fluid Dynamic Analyses of Rocket Based Combined Cycle Engine Flowfields, Ph.D. Thesis, Penn State Univ, 1995.

Escher, W. J. D., Rocket-Based Copmbined-Cycle RBCC Powered Spaceliner Class Vehicles Can Advantageously Employ Vertical Takeoff and Landing (VTOL) AIAA paper 95-6145, 6th Int. Aerospace Plane and Hypersonic Conf., Chattanooga, Tenn., April, 1995.

Foster, R. W., Escher, W. J. D., and Robinson, J., Air Augmented Rocket Propulsion Concepts, AFL-TR-88-004, Jan., 1988.

Heiser, W. H., and Pratt, D. T., Hypersonic Air breath ng Propulsion, AIAA Education Series, 1994.

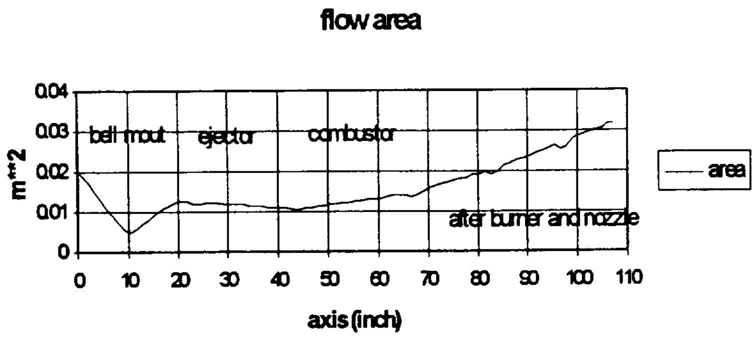

Fig. 1

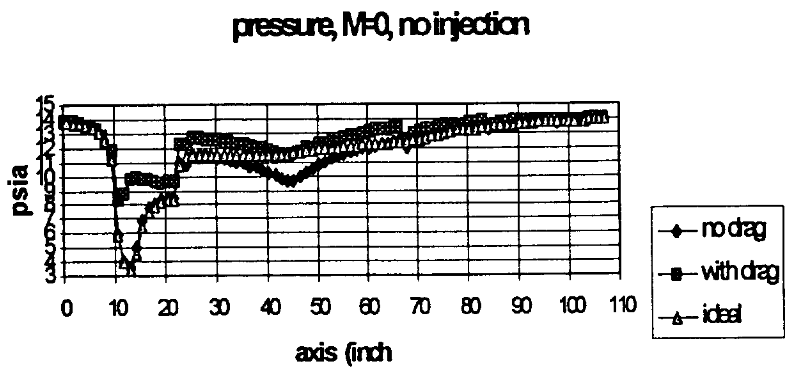

Fig. 2

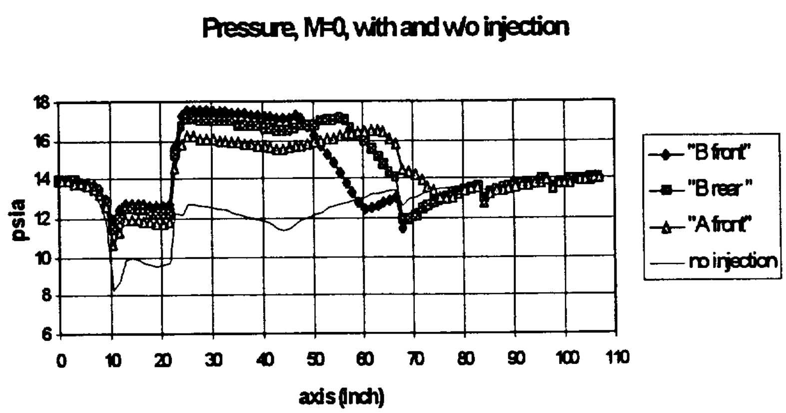

Fig. 3

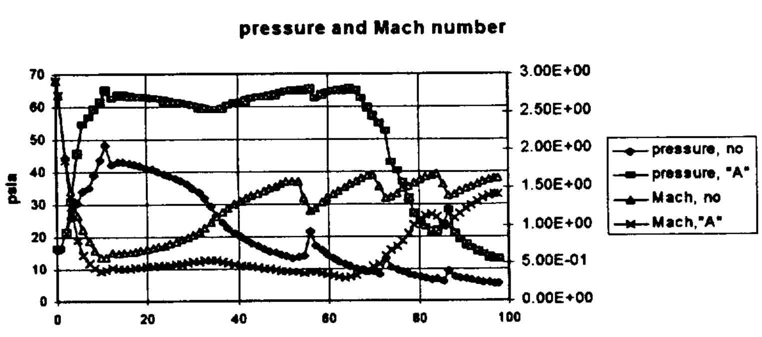

Fig.4